inventions

MDPI

Article

Thermal Aspects of Casson Nanoliquid with Gyrotactic Microorganisms, Temperature-Dependent Viscosity, and Variable Thermal Conductivity: Bio-Technology and Thermal Applications

Kamel Al-Khaled [1] and Sami Ullah Khan [2,*]

[1] Department of Mathematics & Statistics, Jordan University of Science and Technology, P.O. Box 3030, Irbid 22110, Jordan; kamel@just.edu.jo

[2] Department of Mathematics, COMSATS University Islamabad, Sahiwal 57000, Pakistan

* Correspondence: sk_iiu@yahoo.com

Received: 10 July 2020; Accepted: 11 August 2020; Published: 13 August 2020

Abstract: Owing to the expensive applications of nanoparticles in engineering sciences, an admirable attention has been intended by researchers on this topic in recent years. The utilization of nanoparticles as asource of energy is intended much attention of investigators in recent decade. This novel attempt investigates the thermal properties of Casson nanofluid containing microorganisms induced by an oscillatory moving surface. The fundamental features of heat and mass phenomenon are inspected by utilizing the temperature-dependent viscosity. Buongiorno's mathematical model is used to report the famous Brownian motion and thermophoretic diffusion consequences. The flow problem characterizes the partial differential equations for which analytical solution has been computed with a convincible accuracy. The insight physical features are inspected with help of various curves. The physical significances of flow parameters is studied via various graphs.

Keywords: Casson nanofluid; gyrotactic microorganisms; activation energy; temperature dependent viscosity; homotopy analysis method

1. Introduction

The nano-materials, because of their magnificent thermal performances, are recognized as a powerful source of energy and have many applications in modern thermal engineering, technological, and industrial processes. The heat capacity, thermal features, and many physical performances can be significantly improved with utilization of nanoparticles. In fact, the heat transportation process is remarkably affected with low thermal conductivity of many widely used base materials (ethylene glycol, engine oil, water). The nanoparticles are prepared with suspension of base liquids and different metals which have ultrafine thermal conductivity. The heat transfer enhancement in base of nanoparticles is considered as one of themost convenient energy resources in 21st century. Because ofimproved thermal features, the nanofluids have many applications in solar energy, micro-manufacturing, thermal processes, pharmaceutical applications, cancer chemotherapy, cooling mechanisms, chemical industries, and metallurgical applications [1]. The appliances of nano-materials in radiators and automobiles as coolants are more attractive due to better size and favorable expenditures. The basic continuation on this topic was organized by Choi [2] in 1995 which was further extended by famous researchers by using distinct dynamic flow features. The contribution of Boungiorno [3] directed the nanofluid mechanisms procedure based on thermophoresis and Brownian aspects. Turkyilmazoglu [4] analyzed the heat characteristics with nanofluid performances in heated wall jet. Bhatti et al. [5] inspected the nonlinear thermally developed flow of Fe3O4 nanoparticles immersed in base liquid with external

features of slip and thermo-diffusion. The nanofluid flow specified in rotating circular plates with additional magnetic force consequences has been directed by Zhang et al. [6]. Ijaz and Ayub [7] carried out an activation energy applications in Maxwell nanofluid flow by using convective boundary conditions. Shahrestani et al. [8] investigated the heat transfer enhancement in a microchannel filled with Al_2O_3/water nanoparticles. Mahanthesh et al. [9] numerically executed the Hall effects and shape factor of nanoparticles configured by a rotating frame. Hayat et al. [10] scrutinized the Darcy flow of Jeffrey nanofluid with nonlinear radiation prospective. Maleki et al. [11] showed the MAR and artificial neural network applications while examining the thermal consequences of ZnO nano-materials. The Joule heating aspects in dissipative flow of nanofluid with chemical reaction effects was worked out by Shahzad et al. [12]. Ibrahim [13] presented the slip flow of tangent hyperbolic nanoparticles by utilizing convective condition approach. Wang et al. [14] used difference approximation to study the MgO nanoparticles thermal performance. The oscillatory surface flow of micropolar nanofluid with station point phenomenon has been focused by Nadeem et al. [15]. Khan and Shehzad [16] analyzedflow of third grade nanofluid with appliances of analytical approach. Ibrahim and co-researchers [17] employed the modified heat and mass flux relations for tangent hyperbolic nanofluid flow over a moving configuration. Eid and Mabdood [18] investigated the entropy generation analysis for thermally developed flow of micropolar dusty carbon nano-materials under the influence of heat generation features. In another investigation, Eid et al. [19] focused on chemically reactive flow of Carreau nanofluid induced by nonlinear stretched configuration. Al-Hossainy et al. [20] examined the rheological features of Casson nanofluid immersed in porous medium where numerical solution was computed by using famous spectral quasi-linearization numerical scheme with excellent accuracy. The utilization of gold nanoparticles in blood flow of Sisko fluid under the influence of nonlinear thermal radiation and suction/injection aspects was directed by Eid et al. [21]. Boumaiza and co-investigators [22] examined the Falkner-Skan flow of nanoparticles (copper, alumina, and magnetite) in presence of external magnetic force. Eid et al. [23] analyzed the shape factors of nanoparticles in blood flow with additional impact of nonlinear thermal radiation and heat source/sink. An interesting numerical approach namely finite element scheme was followed to simulate the solution. Rehman et al. [24] discussed the heat transfer phenomenon in rotatory flow of magnetized nanoparticles induced by rigid disk. Ragupathi et al. [25] focused on thermal performances of Fe_3O_4 and Al_2O_3nanoparticles flow over a Riga surface. The flow of ferrofluid in a cavity was numerically tackled by Li et al. [26]. Saranya et al. [27] studied the thermal features of ferrofluid subject to the aligned magnetic force. Besthapu et al. [28] utilized the slip effects in stagnation point flow of nanofluid over a convectively heated surface. Abdelmalek et al. [29] investigated the thermally developed flow of viscous nanofluid in grooved computational channel. Rasool et al. [30] analyzed the aspects I entropy generation in flow of Williamson nanofluid over a nonlinear stretched surface. Reddy and Chamkha [31] analyzed the heat transfer enhancement in flow of Al_2O_3–water and TiO_2–water nanoparticles in presence of diffusion-thermo features. RamReddyet al. [32] examined the Soret effects in mixed convection flow of nanofluid with the help of convective boundary conditions. The Falkner-Skan flow of Williamson nanofluid in presence of variable Prandtl number was focused by Basha et al. [33].

The bioconvection phenomenon is another attractive research area thatinvolves a variety of physical applications in real world applications. The bioconvection pattern is referred to the macroscopic convection movement of materials because of density gradient. This fluctuation in density gradient is resulted from the microorganisms communal swimming. Usually such self-propagated microorganisms are pondered in upper liquid region which make it quite denser. The demarcation trend of such lower and upper region surfaces is attributed to the instability of the system. Various biological and medical sciences involves the applications of this phenomenon like enzyme biosensors, bio-fuels, enzymes, transportation processes, micro-systems, bio-technology, biological tissues, bacteria etc. The bioconvection involves applications of microbial-enhanced oil recovery. This phenomenon is based on the collective utilization of nutrients and microorganisms in oil-bearing region to inspect

the permeability variation. Based on directional movement of different microorganisms, the system of bioconvection is characterized into various types like chemotaxis, gyrotactic microorganisms and geotactic microorganisms. Moreover, the idea of nanofluid bioconvection involves diverse significances like automotive coolants, building design, nanoparticles processing, sterilization application in heated sciences, improvement of nanoparticles stability polymer coating etc. The fundamental contribution of nanoparticles bioconvection was led by Kuznetsov [34,35] which was further extended in various directions with help ofdifferent features. Rashad et al. [36] considered the flow of nanofluid containing microorganisms where numerical treatment was performed to simulate the solution. Uddin et al. [37] imposed the multiple slip consequences and blowing constraints to study the bioconvection flow of nano-material in porous layer. The non-Newtonian nanofluid flow with microorganisms with Stefan blowing features has been explored by Amirsom et al. [38]. Khan et al. [39] worked on a bioconvection problem induced by truncated cone with the help of finite difference approach. Zohra et al. [40] examined the magnetized flow of nanofluid with gyrotactic microorganisms with involvement of slip parameters in rotating disk. Zhao et al. [41] performed stability mechanism for nanoparticles with gyrotactic microorganisms. The thermal application based on nanofluid interaction and gyrotactic microorganisms in flow of Sisko fluid with interference of slip constraints was followed by Farooq et al. [42]. Chamkha et al. [43] used nonlinear thermal radiation expressions in bioconvection flow of nanofluid with gyrotactic microorganisms over a vertical surface.

The investigation on non-Newtonian fluids is essential because of several engineering, chemical, biomedical, mechanical, and environmental applications. Such novel applications are involved in mining industries, suspensions, motor oils, lubricants, medicine, blood, and many others. The behavior of each non-Newtonian material is different from each other and much attention is needed to discuss the rheological characteristics of each nonlinear fluid model. Among such fluids, Casson fluid is one thatcharacterizes the shear thinning features. The interesting aspects of Casson fluid model is that is behaves like a solid when shear stress is lower as compared to yield stress. Casson fluid model is pertinent for liquids with rods as solids and also suitable for examining the behavior of ink, molten chocolate, and blood. The flow of Casson fluid under the influence of magnetic force involves extensive applications in various engineering and industrial processes like material polymers, plasma fusion technology, accelerators, magneto-hydrodynamic chemical reactor processing, purification in crude oil, and applications in polymer technology [44–46].

In this theoretical flow model, we present the numerical simulations for flow of Casson nanofluid containinggyrotactic microorganisms in presence of diverse features like variable viscosity, thermal radiation, mixed convection, and activation energy. The thermal radiation features are taken into account in nonlinear form which makes the energy equation more complicated. The flow has been induced by a periodically oscillating stretched surface. The pioneer concept for flow configured by oscillatory stretching surface was presented by Wang [47] in 1988. Later on, some studies regarding flow due to oscillatory stretching surface has been presented by investigators by using different non-Newtonian fluid models [48,49]. However, the bioconvection flow of Casson nanofluid in presence of activation energy, nonlinear thermal radiation, and temperature-dependent viscosity has not been reported yet. The aim of this contribution is to fulfill this research gap. The flow due to accelerated surfaces involvesa variety of applications in rotating and oscillatory systems like swirl generators, rotating electrodes, rotor-stator system, centrifuges, boilers, aircraft engines, turbine engines etc. The distinguish aspects of current investigation are summarized as:

1. Develop an unsteady mathematical model for flow of Casson nanofluid induced by a periodically oscillating stretched surface.
2. The bioconvection aspects of nanoparticles are studied in presence of gyrotactic microorganisms.
3. In current analysis, the viscosity of fluid is assumed to be temperature dependent.
4. The novel features like mixed convection, activation energy, and nonlinear thermal radiation are also utilized to examine the heat and mass transfer phenomenon.

5. The formulated nonlinear partial differential equations are analytically tackled with the help of homotopy analysis method [50–53].
6. The physical consequences for each flow parameter are illustrated graphically.

2. Mathematical Modeling

The flow of Casson nanofluid with gyrotactic microorganisms is considered over an accelerated stretched sheet in theCartesian plane. For two-dimensional flow, u (velocity component) is elongated in x direction while v (velocity component) is configured along the y direction as shown in Figure 1. The problem is modeled upon following flow assumptions:

1. The magnetic force features are taken into account by imposing it in vertical directions. Following to the assumption of very large magnetic diffusivity, the effects of induced magnetic field and Hall current are neglected.
2. The viscosity of fluid is assumed to be temperature dependent by using famous Reynolds exponential concept.
3. The activation energy features are utilizedin the concentration by using Arrhenius relations.
4. The nanofluid temperature, concentration, and gyrotactic microorganisms are symbolizedby T, C, and N, respectively.
5. Let T_w be the surface temperature, C_w is surface concentration, while N_w is for surface motile density.
6. Keeping such flow assumptions in mind, the developed governing equations are [45,46].

$$\frac{\partial u}{\partial x} + \frac{\partial v}{\partial y} = 0, \tag{1}$$

$$\frac{\partial u}{\partial t} + u\frac{\partial u}{\partial x} + v\frac{\partial u}{\partial y} = \left(1 + \frac{1}{\Gamma}\right)\frac{1}{\rho_f}\frac{\partial}{\partial y}\left(\mu^*(T)\frac{\partial u}{\partial y}\right) - \frac{\sigma^{\otimes}B_0^2}{\rho_f}u + \frac{1}{\rho_f}\begin{bmatrix} (1-C_\infty)\rho_f\beta^* g(T-T_\infty) \\ -\left(\rho_p - \rho_f\right)g(C-C_\infty) \\ -(N-N_\infty)g\gamma^*\left(\rho_m - \rho_f\right) \end{bmatrix}, \tag{2}$$

$$\frac{\partial T}{\partial t} + u\frac{\partial T}{\partial x} + v\frac{\partial T}{\partial y} = \left(\alpha_{\otimes} + \frac{16T_\infty^3\sigma_r}{3\left(\rho c_p\right)_f k_r}\right)\frac{\partial^2 T}{\partial y^2} + \Lambda^{\otimes}\left\{D_B\frac{\partial T}{\partial y}\frac{\partial C}{\partial y} + \frac{D_T}{T_\infty}\left(\frac{\partial T}{\partial y}\right)^2\right\}, \tag{3}$$

$$\frac{\partial C}{\partial t} + u\frac{\partial C}{\partial x} + v\frac{\partial C}{\partial y} = D_B\frac{\partial^2 C}{\partial y^2} + \frac{D_T}{T_\infty}\frac{\partial^2 T}{\partial y^2} - K_1 r^2(C-C_\infty)\left(\frac{T}{T_\infty}\right)^2\exp\left(\frac{-E_a}{\kappa T}\right), \tag{4}$$

$$\frac{\partial N}{\partial t} + u\frac{\partial N}{\partial x} + v\frac{\partial N}{\partial y} + \frac{b^{\oplus}w^{\oplus}}{(C_w - C_\infty)}\left[\frac{\partial}{\partial y}\left(N\frac{\partial C}{\partial y}\right)\right] = D_m\left(\frac{\partial^2 N}{\partial y^2}\right), \tag{5}$$

where t is time, μ^* is temperature dependent viscosity, Γ is Casson fluid parameter, β^* coefficient of volume suspension, $\sigma^{\otimes}$ electrical conductivity, $\alpha_{\otimes}$ thermal diffusivity, D_m microorganisms diffusion constant, $\Lambda^{\otimes} = \left(\rho c_p\right)_p / \left(\rho c_p\right)_f$ is effective heat nanoparticles and effective base liquid heat capacity, ν kinematic viscosity B_0 magnetic field strength, g gravity, E_a activation energy, ρ_f fluid density, ρ_p nanoparticles density, K_r reaction rate, ρ_m motile microorganism density, D_B diffusion constant, n rate constant, κ Boltzmann constant,$b^{\oplus}$ chemotaxis constant, $w^{\oplus}$ swimming cells speedand Boltzmann constant (κ).

The relation for temperature-dependent viscosity (μ^*) appeared in Equation (2) is obtained by following Reynolds number exponential equation

$$\mu^*(\theta) = e^{-(\delta\theta)} = 1 - (\delta\theta) + O\left(\delta^2\right), \tag{6}$$

where δ is viscosity vector. The boundary conditions for above constituted equations are:

$$u = u_\omega = bx\sin\omega t, v = 0,\ T = T_w,\ C = C_w, N = N_w \text{ at } y = 0,\ t > 0, \tag{7}$$

$$u \to 0,\ \frac{\partial u}{\partial y} \to 0, T \to T_\infty, C \to C_\infty, N \to N_\infty \text{ at } y \to \infty. \tag{8}$$

The appropriate variables thataltered the above equations in dimensionless form are given as thefollowing relations [47–49]:

$$\eta = \sqrt{\frac{b}{\nu}}y,\ \tau = t\omega,\ u = bxf_y(\eta,\tau),\ v = -\sqrt{\nu b}f(\eta,\tau), \tag{9}$$

$$\theta(\eta,\tau) = \frac{T - T_\infty}{T_w - T_\infty},\ \varphi(\eta,\tau) = \frac{C - C_\infty}{C_w - C_\infty},\ \chi(\eta,\tau) = \frac{N - N_\infty}{N_w - N_\infty}, \tag{10}$$

where θ is the dimensionless temperature profile, ϕ is the concentration profile, χ represents the dimensionless motile microorganism, and τ is dimensionless time.

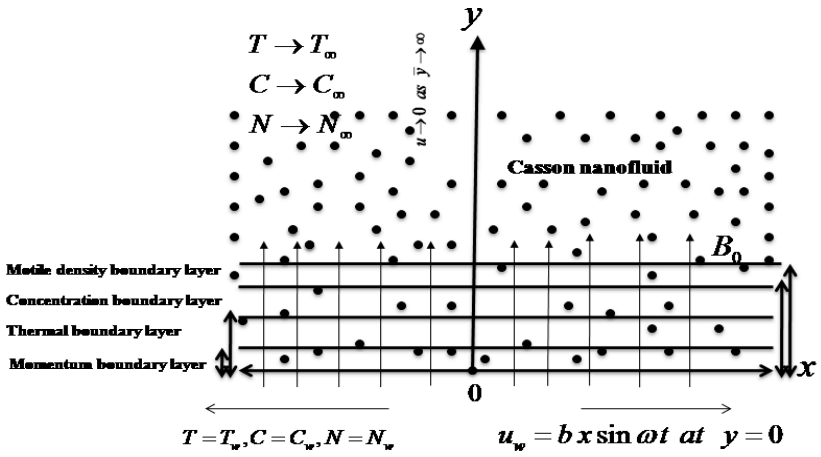

Figure 1. Geometry of problem.

Following set of dimensionless equations are achieved by using above relations in governing equations

$$\left(1 + \frac{1}{\Gamma}\right)\left[(1 - (\delta\theta))f_{\eta\eta\eta} - \delta\theta_\eta f_{\eta\eta}\right] - Sf_{y\tau} - f_y^2 - \Omega f_y + ff_{yy} + \lambda(\theta - Nr\varphi - Rb\chi) = 0, \tag{11}$$

$$\left[1 + \tfrac{4}{3}Rd\{1 + (\theta_w - 1)\theta\}^3\right]\theta_{\eta\eta} + Rd\left[3(\theta_w - 1)\theta_\eta^2\right][1 + (\theta_w - 1)\theta]^2 + \Pr\left[\begin{array}{l} -S\phi_\tau + f\phi_\eta \\ +Nb\theta_\eta\phi_\eta + Nt\left(\theta_\eta\right)^2 \end{array}\right] = 0, \tag{12}$$

$$\varphi_{\eta\eta} + \frac{Nt}{Nb}\theta_{\eta\eta} - S(Sc)\varphi_\tau + Scf\varphi_\eta - (Sc)\sigma(1 + \delta^*\theta)^n \exp\left(\frac{-E}{(1 + \delta^*\theta)}\right)\varphi = 0, \tag{13}$$

$$\chi_{\eta\eta} - S(Lb)\chi_\tau + Lb\chi_\eta - Pe\left[\varphi_{\eta\eta}(\chi + \varpi) + \chi_\eta\varphi_\eta\right] = 0, \tag{14}$$

The boundary conditions are

$$f_\eta(0,\ \tau) = \sin\tau,\ f(0,\ \tau) = 0,\ \theta(0,\tau) = 1, \varphi(0,\tau) = 1, \chi(0,\tau) = 1, \tag{15}$$

$$f_\eta(\infty,\ \tau) \to 0,\ \theta(\infty,\tau) \to 0, \varphi(\infty,\tau) \to 0, \chi(\infty,\tau) \to 0, \tag{16}$$

The dimensionless flow parameters are oscillating frequency to stretching rate ratio parameter (S), mixed convection parameter (λ), Hartmann number (Ω), Brownian motion parameter (Nb), bioconvection Rayleigh number (Rb), buoyancy ratio constant (Nr), Prandtl number $(\Pr)$, microorganisms concentration difference (ϖ), reaction constant (σ), Lewis number (Le), thermophoresis parameter (Nt), activation energy constant (E), Peclet number (Pe) and bioconvection Lewis number (Lb) which are mathematically defined as:

$S = \omega/b$, $\Omega = \sigma^{\otimes}B_0^2/\rho_f b$, $\lambda = \beta^* g(1-C_\infty)(T_w - T_\infty)/b^2 x$, $\mathrm{Pr} = \nu/\alpha_{\otimes}$, $Nb = \Lambda^{\otimes} D_B(C_w - C_\infty)/\nu$, $Nr = \left(\rho_p - \rho_f\right)(C_w - C_\infty)/\beta^*\rho_f(1-C_\infty)T_\infty$, $\varpi = N_\infty/(N^*{}_w - N^*_\infty)$, $Lb = \nu/D_m$, $E = \frac{E^*}{kT_\infty}$, $Rb = \gamma^*(N_w - N_\infty)\left(\rho_m - \rho_f\right)/\beta^*\rho_f(1-C_\infty)(T_w - T_\infty)$, $Nt = \Lambda^{\otimes} D_T(T_w - T_\infty)/T_\infty\nu$, $Pe = b_1 w_c/D_m$, $Pe = b^{\oplus}w^{\oplus}/D_m$.

The skin friction force is related as:

$$C_f = \frac{(\tau_w)_{y=0}}{\rho_f u_w^2}, \tag{17}$$

In view of Equations (9) and (10), Equation (17) yields [45,46]

$$\mathrm{Re}_x^{1/2} C_f = \left(1 + \frac{1}{\Gamma}\right) f_{\eta\eta}(0,\tau). \tag{18}$$

We define local Nusselt number Nu_x as follows [45,46]

$$\left.\begin{aligned} Nu_x &= \tfrac{xq_h}{k(T_w - T_\infty)}, q_h = -k\left(\tfrac{\partial T}{\partial y}\right)_{(0,\tau)} + (qr)_w, \\ Sh_x &= \tfrac{xq_s}{D_B(C_w - C_\infty)}, q_s = -D_B\left(\tfrac{\partial C}{\partial y}\right)_{(0,\tau)}, \\ Nn_x &= \tfrac{xq_n}{D_n(N_w - N_\infty)}, q_n = -D_m\left(\tfrac{\partial N}{\partial y}\right)_{(0,\tau)}, \end{aligned}\right\} \tag{19}$$

where k is thermal conductivity, q_h heat flux at wall, q_s is the mass flux, q_n denotes the motilemicroorganism flux, and Re_x is the local Reynolds number. In view of Equations (9) and (10), Equation (19) becomes

$$\left.\begin{aligned} \tfrac{Nu_x}{\sqrt{\mathrm{Re}_x}} &= -\left(1 + \tfrac{4}{3}Rd\theta_w^3(0,\tau)\right), \\ \tfrac{Sh_x}{\sqrt{\mathrm{Re}_x}} &= -\varphi_\eta(0,\tau), \\ \tfrac{Nn_x}{\sqrt{\mathrm{Re}_x}} &= -\chi_\eta(0,\tau). \end{aligned}\right\} \tag{20}$$

where Nu_x is local Nusselt number, Sh_x is local Sherwood number, and Nn_x is the local motile density number.

3. Homotopy Analysis Method

The proper initial guesses are

$$f_0(\eta,\tau) = \sin\tau - e^{-\eta},\ \theta_0(\eta) = e^{-\eta},\ \varphi_0(\eta) = e^{-\eta}, \chi_0(\eta) = e^{-\eta}. \tag{21}$$

The auxiliary linear operators are defined as

$$\pounds_f = \frac{\partial^3}{\partial\eta^3} - \frac{\partial}{\partial\eta},\ \pounds_\theta = \frac{\partial^2}{\partial\eta^2} - 1,\ \pounds_\varphi = \frac{\partial^2}{\partial\eta^2} - 1, \pounds_\chi = \frac{\partial^2}{\partial\eta^2} - 1, \tag{22}$$

which satisfy

$$\pounds_f[c_1 + c_2 e^{\eta} + c_3 e^{-\eta}] = 0, \tag{23}$$

$$\pounds_\theta[c_4 e^{\eta} + c_5 e^{-\eta}] = 0, \tag{24}$$

$$\pounds_\phi[c_6 e^{\eta} + c_7 e^{-\eta}] = 0, \tag{25}$$

$$\pounds_\chi[c_8 e^{\eta} + c_9 e^{-\eta}] = 0, \tag{26}$$

where $c_i (i = 1,\ 2, \ldots, 9)$ represents arbitrary constants.

4. Convergence Analysis

The convergence procedure of series solution computed via HAM is strictly based upon the favorable selection of $h_f, h_\theta h_\phi$, and h_χ (auxiliary parameters). This task is completed by sketching Figure 2 where h-curvesareplottedfor different values of flow parameters. The resulted values convey that a good accuracy of solution is achieved when $-1.6 \leq h_f \leq -0.2$, $-1.6 \leq h_\theta \leq 0.0$, $-1.1 \leq h_\phi \leq 0$ and $-1 \leq h_\chi \leq 0$.

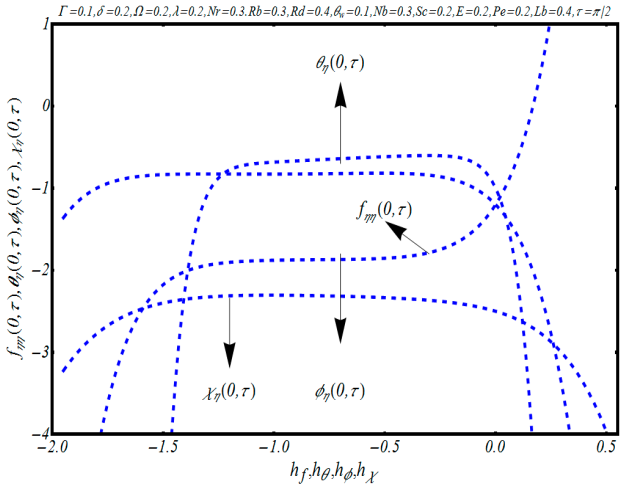

Figure 2. Curves for $f_{\eta\eta}, \theta_\eta, \phi_\eta$ and χ_η.

5. Solution Verification

The solution is verified by comparing the present results with Abbas et al.'s [48] as a limiting case in Table 1. A convincible accuracy of both solutions is obtained.

Table 1. Comparison of $f_{\eta\eta}(0,\tau)$ with [48] when $S = 1, \Gamma \to \infty$, $\Omega = 0, \delta = 0, \lambda = 0, Nr = 0$ and $Rb = 0$.

τ	Abbas et al. [48]	Present Results
$\tau = 1.5\pi$	11.678656	11.678657
$\tau = 5.5\pi$	11.678707	11.678708
$\tau = 9.5\pi$	11.678656	11.678656

6. Discussion

The physical visualization for involved flow parameters is quite necessary to convey the real application of formulated problem in various industrial and engineering processes. On this end, various graphs are sketched fordifferent flow parameters like oscillating frequency to stretching rate ratio (S), mixed convection parameter (λ), buoyancy ratio constant (Nr), Hartmann number (Ω), Brownian motion parameter (Nb), bioconvection Rayleigh number (Rb), Prandtl number (Pr), microorganisms concentration difference (ϖ), (δ_1), reaction constant (δ^*), Lewis number (Le), thermophoresis parameter (Nt), activation energy constant (E), Peclet number (Pe), and bioconvection Lewis number (Lb) for dimensionless nanofluid temperature θ, concentration distribution ϕ, and microorganisms χ. Figure 3a reports the change in nanofluid temperature θ for diverse Hartmann number Ω and Casson fluid parameter Γ. The temperature profile increases with increment of both parameters. Physically, Hartmann number is alternatively related to a resistive nature Lorentz force thatresists the fluid motion effectively, which producesresistancebetween fluid particles due to which θ increases. Furthermore, thicker thermal boundary layer is noticed with increment of Ω. The Casson fluid parameter also plays a significant contribution to improve the nanofluid temperature. The physical aspects of such increasing trend are justified as larger values of Casson fluid parameter increase the viscosity nature

of the flow which increases the temperature profile. Therefore, the consideration of non-Newtonian fluid (Casson fluid) is more useful to improve the heat transportation process. The onset of two important nanofluid parameters namely thermophoresis parameter Nt and Brownian constant Nb on θ is examined in Figure 3b. A rise profile of θ is associated with both Nt and Nb. The physical aspects behind such enhancing behavior of θ is more prominent for Nt. The thermophoresis phenomenon contains the migrated heated fluid particles in the region of cold surface. In fact, the heated fluid particles move from hot region to cold surface because of temperature gradient. This migration procedure helps to improve the nanofluid temperature. Similarly, the Brownian motion contains the random fluid particles motion within the fluid system which improves the temperature when Nb is maximum. The graphical trend of θ for Nr and Rb is observed in Figure 3c. Since both parameters involve the buoyancy forces which attribute to the increment in θ. Figure 3d utilizes the variation in θ for different values of Prandtl number Pr and viscosity parameter δ. The curve of θ decreases with larger values of Pr. Physically, higher Pr is referred to low thermal diffusivity which helps to reduce the nanofluid temperature. The thermal boundary layer becomes thinner with increasing Pr. On the other hand, the higher values of δ result in a progressive nanofluid temperature. It is emphasized that the consideration of variationviscosity in the enhancement of nanofluid temperature is more efficient as compared to traditional base fluid viscosity. The impact of radiation parameter Rd and heat source parameter θ_w on θ is shownin Figure 3e. The temperature θ increases with increasing values of both parameters. The thermal radiation phenomenon conveys special fundamental thermal applications in many engineering, industrial, chemical, mechanical, and processing processes. It is further remarked that the consideration of nonlinear thermal radiation is more effective to improve the heating/cooling processes.

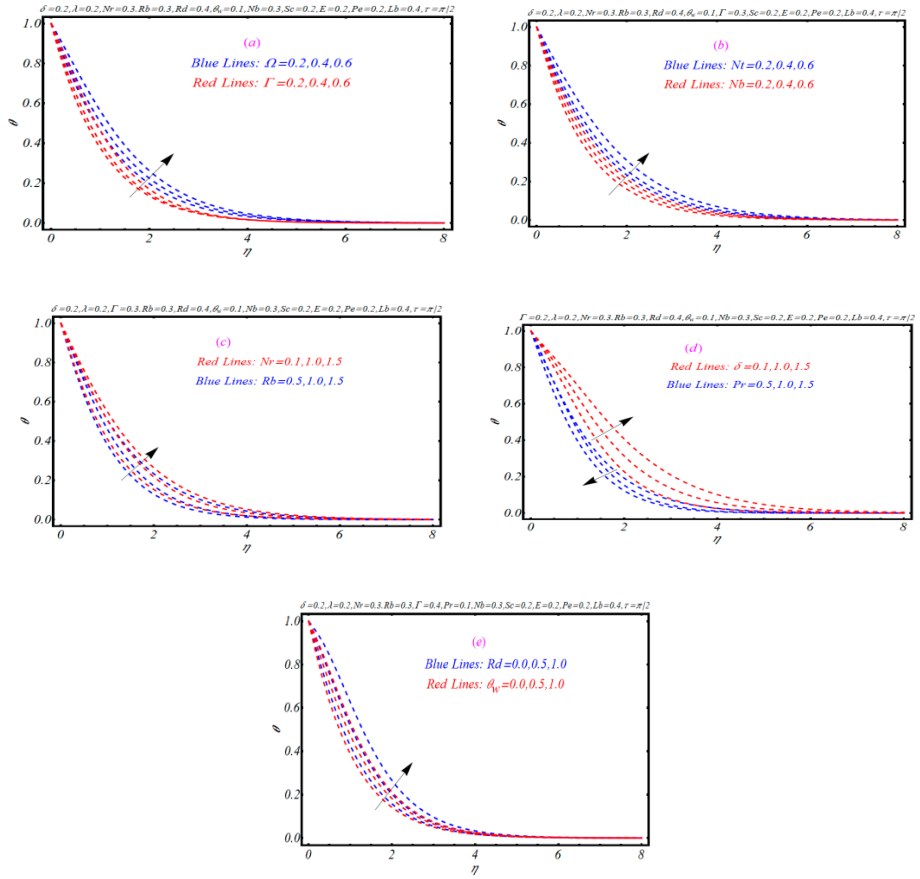

Figure 3. Variation in θ for (**a**) Ω and Γ, (**b**) Nt and Nb, (**c**) Nr and Rb, (**d**) Pr and δ, (**e**) Rd and θ_w.

Figure 4a–cpresents the variation in concentration profile ϕ for different values of thermophoresis parameter Nt, Casson fluid parameter Γ, ratio of oscillating frequency to stretching rate S, Hartmann number Ω, buoyancy ratio constant Nr, and activation energy parameter E. Figure 4a claims the influence of Nt and Γ on ϕ. A larger profile of ϕ is noted for both parameters. The increment in concentration profile ϕ is referred to the viscous nature of Casson liquid. It is also analyzed that concentration boundary layer thickness is more thicker for Nt as compared to Γ. Figure 4b utilizes the physical aspects of oscillating frequency to stretching rate ratio parameter S and Hartmann number Ω on ϕ. The concentration of nanofluid increases when S and Ω are maximum. The Lorentz forces become more dominant when Hartmann number Ω gets maximum values. Figure 4c is prepared to see the physical consequences of buoyancy ratio constant Nr and activation energy parameter E on ϕ. Again ϕ shows an increasing variation when both parameters get leading numerical values. The activation energy is the minimum energy amount required to initiate the concentration process. More activation energy provides an enhanced concentration field. The increment in ϕ due to Nr is justified because ofthe involvement of buoyancy forces.

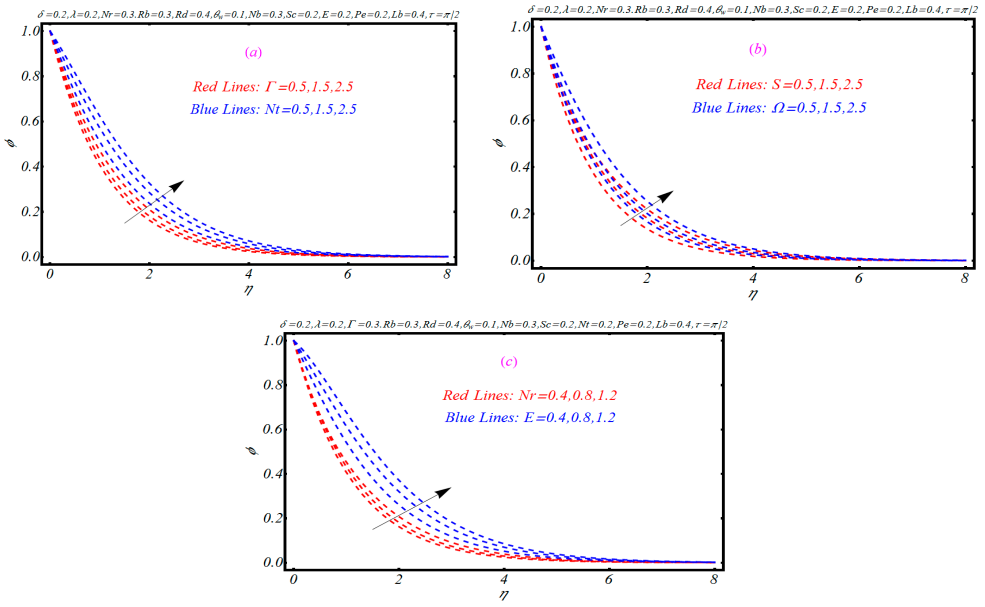

Figure 4. Variation in ϕ for (**a**) Nt and Γ, (**b**) S and Ω, (**c**) Nr and E.

In order to see the change in microorganism field χ against bioconvection Lewis number Lb, Peclet number Pe, Casson fluid parameter Γ, and bioconvection Rayleigh number Rb, Figure 5a,b is prepared. It is noted that χ decreases with larger variation of Lb and Pe (Figure 5a). The motile boundary layer thickness becomes thinner by increasing Pe. Physically, an increasing numerical value of Pe reduces the motile density which declines the microorganism field χ. Figure 5b communicates the change in χ for Γ and Rb. Here χ shows increasing trend with both parameter.

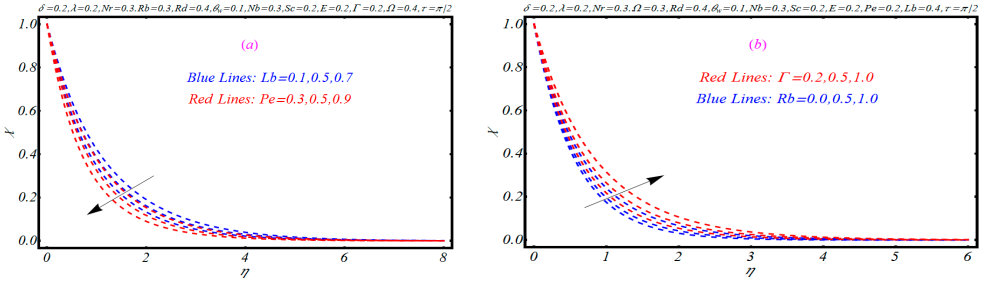

Figure 5. Variation in χ for (**a**) Lb and Pe, (**b**) Γ and Rb.

Figure 6a,b presents thevariation of $\mathrm{Re}_x^{1/2}C_f$ against τ for Casson fluid parameter Γ and viscosity parameter δ. An increased periodic oscillation of wall shear stress with uniform frequency is observed when both parameters vary. In both curves, no phase shift is found. Moreover, amplitude of oscillation is more progressive for δ. Such periodic behavior of wall shear force is attributed to the periodic nature of moving stretched surface.

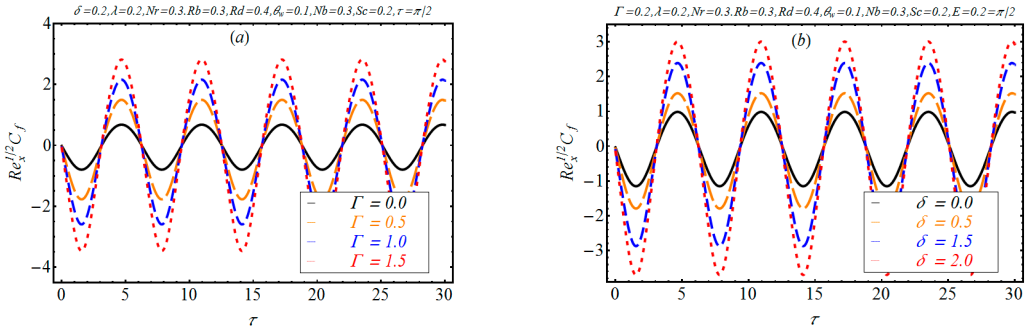

Figure 6. Variation in $\mathrm{Re}_x^{1/2}C_f$ for (**a**) Γ and (**b**) δ.

Table 2 aims to examine the change in local Nusselt number, local Sherwood number, and motile density number against different flow parameters. An increased variation in all these quantities is noticedbecause of the mixed convection parameter λ, viscosity parameter α, and Prandtl number Pr while opposite numerical values are achieved for Hartmann number Ω and buoyancy ratio constant Nr.

Table 2. Illustration of $-\theta_\eta(0,\tau)$, $-\varphi_\eta(0,\tau)$ and $-\chi_\eta(0,\tau)$ for different flow parameters when $\tau = \pi/2$.

δ	Nr	Rb	Γ	Ω	λ	$-\theta_\eta(0,\tau)$	$-\varphi_\eta(0,\tau)$	$-\chi_\eta(0,\tau)$
0.2						0.45639	0.42355	0.57866
0.4	0.3	0.1	0.3	0.5	0.5	0.43208	0.41327	0.55554
0.6						0.41438	0.40768	0.53154
	0.2					0.50523	0.47764	0.55657
0.1	0.4					0.47768	0.44542	0.52098
	0.6					0.45455	0.41457	0.50896
		0.2				0.51214	0.44458	0.54811
		0.4				0.48365	0.42898	0.53632
		0.6				0.45456	0.40624	0.51614
			0.2			0.50256	0.46384	0.57213
			0.4			0.47248	0.43657	0.54112
			0.6			0.42695	0.41468	0.525333
				0.2		0.52659	0.44128	0.55526
				0.4		0.47647	0.426589	0.53456
				0.6		0.44892	0.39321	0.505254
					0.2	0.51653	0.47486	0.55546
					0.4	0.54895	0.51559	0.565478
					0.6	0.57035	0.53236	0.59598

7. Final Remarks

The thermal transportation in bioconvection flow of Casson nanofluid with nonlinear thermal radiation, temperature dependent viscosity, and activation energy is investigated in this work. The analytical approach is followed to predict the solution of modeled flow equations. The physical insight analysis is graphically performed for involved flow parameters. The results are summarized as:

1. The temperature-dependent viscosity, thermophoresis parameter, and Casson fluid parameter effectively improve the nanofluid temperature.

2. The radiation parameter and heating source constant increases the temperature profile.
3. Presence of activation energy and Casson fluid parameter improves the concentration field of nano-materials.
4. The increment in Peclet number bioconvection and Lewis number declined microorganisms field while this physical quantity get maximum variation with Casson fluid parameter and bioconvection Rayleigh number.
5. The wall shear force oscillates with time which increases for viscosity parameter and Casson fluid parameter.
6. The results from the present flow model havevarious fundamental applications in solar energy systems, heat transfer enhancement, cooling and heating processes, environmental applications, thermal engineering, bio-sensors, enzymes, energy consumptions, bio-fuels applications and bio-technology.
7. The obtained results can be further extended for different non-Newtonian fluid models by performing the stability analysis and utilizing distinct features like entropy generation, Joule heating, variable thermal conductivity, porous medium etc.

Author Contributions: S.U.K. formulate the flow problem and literature. K.A.-K. computed the analytical solution of problem and also included physical explanations of flow parameters. All authors have read and agreed to the published version of the manuscript.

Funding: This research received no external funding

Conflicts of Interest: The authors declare no conflict of interest.

Nomenclature

(u, v)	Velocity component
C	Concentration
T_w	Surface temperature
N_w	Surface motile density
μ^*	Temperature dependent viscosity
β^*	Coefficient of volume suspension
$\alpha_\otimes$	Thermal diffusivity
ν	Knematic viscosity
$\Lambda^\otimes$	Effective heat nanoparticles and effective base liquid heat capacity
E_a	Activation energy
ρ_p	Nanoparticles density
ρ_m	Motile microorganism density
n	Rate constant
$b^\oplus$	Chemotaxis constant
κ	Boltzmann constant
θ	Dimensionless temperature profile
S	oscillating frequency to stretching rate ratio
Ω	Hartmann number
Rb	Bioconvection Rayleigh number
Pr	Prandtl number
σ	Reaction constant
Nt	Thermophoresis parameter
Pe	Peclet number
k	Thermal conductivity
q_s	Mass flux
Re_x	Local Reynolds number
Sh_x	Local Sherwood number
T	Temperature
ρ_f	Fluid density
K_r	Reaction rate

D_B	Diffusion constant
κ	Boltzmann constant
$w^{\oplus}$	Swimming cells speed
ϕ	Concentration profile
χ	Motile microorganism
λ	Mixed convection parameter
Nb	Brownian motion parameter
Nr	Buoyancy ratio constant
ϖ	microorganisms concentration difference
Le	Lewis number
E	activation energy constant
Lb	Bioconvection Lewis number
q_h	Heat flux at wall
q_n	Motile microorganism flux
Nu_x	Local Nusselt number
Nn_x	Local motile density number
N	Gyrotactic microorganisms
C_w	surface concentration
t	Time
Γ	Casson fluid parameter
$\sigma^{\otimes}$	Electrical conductivity
D_m	Microorganisms diffusion constant
B_0	Magnetic field strength
g	Gravity

References

1. Afzal, K.; Aziz, A. Transport and heat transfer of time dependent MHD slip flow of nanofluids in solar collectors with variable thermal conductivity and thermal radiation. *Results Phys.* **2016**, *6*, 746–753. [CrossRef]
2. Choi, S.U.S. Enhancing thermal conductivity of fluids with nanoparticles. *ASME Publ. Fed.* **1995**, *231*, 99–106.
3. Buongiorno, J. Convective Transport in Nanofluids. *J. Heat Transf.* **2005**, *128*, 240–250. [CrossRef]
4. Turkyilmazoglu, M. Flow of nanofluid plane wall jet and heat transfer. *Eur. J. Mech. B Fluids* **2016**, *59*, 18–24. [CrossRef]
5. Bhatti, M.M.; Khalique, C.M.; Bég, T.A.; Bég, O.A.; Kadir, A. Numerical study of slip and radiative effects on magnetic Fe_3O_4-water-based nanofluid flow from a nonlinear stretching sheet in porous media with Soret and Dufour diffusion. *Mod. Phys. Lett. B* **2019**, *34*, 2050026. [CrossRef]
6. Zhang, L.; Arain, M.B.; Bhatti, M.; Zeeshan, A.; Hal-Sulami, H. Effects of magnetic Reynolds number on swimming of gyrotactic microorganisms between rotating circular plates filled with nanofluids. *Appl. Math. Mech.* **2020**, *41*, 637–654. [CrossRef]
7. Ijaz, M.; Ayub, M. Nonlinear convective stratified flow of Maxwell nanofluid with activation energy. *Heliyon* **2019**, *5*, e01121. [CrossRef]
8. Shahrestani, M.I.; Maleki, A.; Shadloo, M.S.; Tlili, I. Numerical Investigation of Forced Convective Heat Transfer and Performance Evaluation Criterion of Al_2O_3/Water Nanofluid Flow inside an Axisymmetric Microchannel. *Symmetry* **2020**, *12*, 120. [CrossRef]
9. Mahanthesh, B.; Amala, S.; Gireesha, B.J.; Animasaun, I.L. Effectiveness of exponential heat source, nanoparticle shape factor and Hall current on mixed convective flow of nanoliquids subject to rotating frame. *Multidiscip. Model. Mater. Struct.* **2019**, *15*, 758–778. [CrossRef]
10. Hayat, T.; Bibi, F.; Farooq, S.; Khan, A.A. Nonlinear radiative peristaltic flow of Jeffrey nanofluid with activation energy and modified Darcy's law. *J. Braz. Soc. Mech. Sci. Eng.* **2019**, *41*, 296. [CrossRef]
11. Maleki, A.; Elahi, M.; Assad, M.E.H.; Nazari, M.A.; Shadloo, M.S.; Nabipour, N. Thermal conductivity modeling of nanofluids with ZnO particles by using approaches based on artificial neural network and MARS. *J. Therm. Anal. Calorim.* **2020**, 1–12. [CrossRef]
12. Shahzad, F.; Sagheer, M.; Hussain, S. MHD tangent hyperbolic nanofluid with chemical reaction, viscous dissipation and Joule heating effects. *AIP Adv.* **2019**, *9*, 025007. [CrossRef]

13. Ibrahim, W. Magnetohydrodynamics (MHD) flow of a tangent hyperbolic fluid with nanoparticles past a stretching sheet with second order slip and convective boundary condition. *Results Phys.* **2017**, *7*, 3723–3731. [CrossRef]
14. Wang, N.; Maleki, A.; Nazari, M.A.; Tlili, I.; Shadloo, M.S. Thermal Conductivity Modeling of Nanofluids Contain MgO Particles by Employing Different Approaches. *Symmetry* **2020**, *12*, 206. [CrossRef]
15. Nadeem, S.; Ullah, N.; Khan, A.U. Impact of an oblique stagnation point on MHD micropolar nanomaterial in porous medium over an oscillatory surface with partial slip. *Phys. Scr.* **2019**, *94*, 065209. [CrossRef]
16. Khan, S.U.; Shehzad, S.A. Brownian movement and thermophoretic aspects in third grade nanofluid over oscillatory moving sheet. *Phys. Scr.* **2019**, *94*, 095202. [CrossRef]
17. Ibrahim, W.; Gizewu, T. Tangent hyperbolic nanofluid with mixed convection flow: An application of improved Fourier and Fick's diffusion model. *Heat Transf. Asian Res.* **2019**, *48*, 4217–4239. [CrossRef]
18. Eid, M.R.; Mabood, F. Entropy analysis of a hydromagnetic micropolar dusty carbon NTs-kerosene nanofluid with heat generation: Darcy-Forchheimer scheme. *J. Therm. Anal. Calorim.* **2020**, 1–18. [CrossRef]
19. Eid, M.R.; Mahny, K.; Dar, A.; Muhammad, T. Numerical study for Carreau nanofluid flow over a convectively heated nonlinear stretching surface with chemically reactive species. *Phys. A Stat. Mech. Appl.* **2020**, *540*, 123063. [CrossRef]
20. Al-Hossainy, A.F.; Eid, M.R.; Zoromba, M.S. SQLM for external yield stress effect on 3D MHD nanofluid flow in a porous medium. *Phys. Scr.* **2019**, *94*, 105208. [CrossRef]
21. Eid, M.R. Effects of NP Shapes on Non-Newtonian Bio-Nanofluid Flow in Suction/Blowing Process with Convective Condition: Sisko Model. *J. Non-Equilib.* **2020**, *45*, 97–108. [CrossRef]
22. Boumaiza, N.; Kezzar, M.; Eid, M.R.; Tabet, I. On numerical and analytical solutions for mixed convection Falkner-Skan flow of nanofluids with variable thermal conductivity. *Waves Random Complex Media* **2019**, 1–20. [CrossRef]
23. Eid, M.R.; Al-Hossainy, A.F.; Zoromba, M.S. FEM for Blood-Based SWCNTs Flow Through a Circular Cylinder in a Porous Medium with Electromagnetic Radiation. *Commun. Theor. Phys.* **2019**, *71*, 1425. [CrossRef]
24. Rehman, K.U.; Shahzadi, I.; Malik, M.; Al-Mdallal, Q.; Zahri, M. On heat transfer in the presence of nano-sized particles suspended in a magnetized rotatory flow field. *Case Stud. Therm. Eng.* **2019**, *14*, 100457. [CrossRef]
25. Ragupathi, P.; Abdul Hakeem, A.K.; Al-Mdallal, Q.M.; Ganga, B.; Saranya, S. Non-uniform heat source/sink effects on the three-dimensional flow of Fe_3O_4/Al_2O_3 nanoparticles with different base fluids past a Riga plate. *Case Stud. Therm. Eng.* **2019**, *15*, 100521. [CrossRef]
26. Li, Z.; Shafee, A.; Ramzan, M.; Rokni, H.B.; Al-Mdallal, Q.M. Simulation of natural convection of Fe_3O_4-water ferrofluid in a circular porous cavity in the presence of a magnetic field. *Eur. Phys. J. Plus* **2019**, *134*, 77. [CrossRef]
27. Saranya, S.; Al-Mdallal, Q. Non-Newtonian ferrofluid flow over an unsteady contracting cylinder under the influence of aligned magnetic field. *Case Stud. Therm. Eng.* **2020**, 100679. [CrossRef]
28. Besthapu, P.; Haq, R.U.; Bandari, S.; Al-Mdallal, Q. Thermal radiation and slip effects on MHD stagnation point flow of non-Newtonian nanofluid over a convective stretching surface. *Neural Comput. Appl.* **2017**, *31*, 207–217. [CrossRef]
29. Abdelmalek, Z.; Rehman, K.U.; Al-Mdallal, Q.; Al-Kouz, W.; Malik, M. Dynamics of thermally magnetized grooved flow field having uniformly heated circular cylinder: Finite element analysis. *Case Stud. Therm. Eng.* **2020**, 100718. [CrossRef]
30. Rasool, G.; Zhang, T.; Chamkha, A.J.; Shafiq, A.; Tlili, I.; Shahzadi, G. Entropy Generation and Consequences of Binary Chemical Reaction on MHD Darcy–Forchheimer Williamson Nanofluid Flow Over Non-Linearly Stretching Surface. *Entropy* **2019**, *22*, 18. [CrossRef]
31. Reddy, P.S.; Chamkha, A.J. Soret and Dufour effects on MHD convective flow of Al_2O_3-water and TiO_2-water nanofluids past a stretching sheet in porous media with heat generation/absorption. *Adv. Powder Technol.* **2016**, *27*, 1207–1218. [CrossRef]
32. Ramreddy, C.; Murthy, P.S.; Chamkha, A.J.; Rashad, A.M. Soret effect on mixed convection flow in a nanofluid under convective boundary condition. *Int. J. Heat Mass Transf.* **2013**, *64*, 384–392. [CrossRef]
33. Basha, H.T.; Sivaraj, R.; Reddy, A.S.; Chamkha, A.J.; Tilioua, M. Impacts of temperature-dependent viscosity and variable Prandtl number on forced convective Falkner–Skan flow of Williamson nanofluid. *SN Appl. Sci.* **2020**, *2*, 1–14. [CrossRef]

34. Kuznetsov, A. The onset of nanofluid bioconvection in a suspension containing both nanoparticles and gyrotactic microorganisms. *Int. Commun. Heat Mass Transf.* **2010**, *37*, 1421–1425. [CrossRef]
35. Kuznetsov, A.V. Nanofluid bioconvection in water-based suspensions containing nanoparticles and oxytactic microorganisms: Oscillatory instability. *Nanoscale Res. Lett.* **2011**, *6*, 100. [CrossRef]
36. Mallikarjuna, B.; Rashad, A.M.; Chamkha, A.J.; Abdou, M. Mixed bioconvection flow of a nanofluid containing gyrotactic microorganisms past a vertical slender cylinder. *Front. Heat Mass Transf.* **2018**, *10*, 21. [CrossRef]
37. Uddin, M.J.; Alginahi, Y.; Bég, O.A.; Kabir, M.N. Numerical solutions for gyrotactic bioconvection in nanofluid-saturated porous media with Stefan blowing and multiple slip effects. *Comput. Math. Appl.* **2016**, *72*, 2562–2581. [CrossRef]
38. Amirsom, N.A.; Uddin, M.J.; Ismail, A.I.M. MHD boundary layer bionanoconvective non-Newtonian flow past a needle with Stefan blowing. *Heat Transf. Asian Res.* **2018**, *48*, 727–743. [CrossRef]
39. Khan, W.A.; Rashad, A.M.; Abdou, M.; Tlili, I. Natural bioconvection flow of a nanofluid containing gyrotactic microorganisms about a truncated cone. *Eur. J. Mech. B Fluids* **2019**, *75*, 133–142. [CrossRef]
40. Zohra, F.T.; Uddin, M.; Basir, F.; Ismail, A.I.M. Magnetohydrodynamic bio-nano-convective slip flow with Stefan blowing effects over a rotating disc. *Proc. Inst. Mech. Eng. Part N J. Nanomater. Nanoeng. Nanosyst.* **2019**. [CrossRef]
41. Zhao, M.; Xiao, Y.; Wang, S. Linear stability of thermal-bioconvection in a suspension of gyrotactic micro-organisms. *Int. J. Heat Mass Transf.* **2018**, *126*, 95–102. [CrossRef]
42. Farooq, S.; Hayat, T.; Alsaedi, A.; Ahmad, B. Numerically framing the features of second order velocity slip in mixed convective flow of Sisko nanomaterial considering gyrotactic microorganisms. *Int. J. Heat Mass Transf.* **2017**, *112*, 521–532. [CrossRef]
43. Chamkha, A.; Rashad, A.M.; Kameswaran, P.K.; Abdou, M.M.M. Radiation Effects on Natural Bioconvection Flow of a Nanofluid Containing Gyrotactic Microorganisms Past a Vertical Plate with Streamwise Temperature Variation. *J. Nanofluids* **2017**, *6*, 587–595. [CrossRef]
44. Hayat, T.; Shafiq, A.; Alsaedi, A. Effect of Joule Heating and Thermal Radiation in Flow of Third Grade Fluid over Radiative Surface. *PLoS ONE* **2014**, *9*, e83153. [CrossRef]
45. Khan, S.U.; Ali, N.; Mushtaq, T.; Rauf, A.; Shehzad, S.A. Numerical Computations on Flow and Heat Transfer of Casson Fluid over an Oscillatory Stretching Surface with Thermal Radiation. *Therm. Sci.* **2019**, *23*, 3365–3377.
46. Bhatti, M.; Khan, S.U.; Bég, O.A.; Kadir, A. Differential transform solution for Hall and ion-slip effects on radiative-convective Casson flow from a stretching sheet with convective heating. *Heat Transf.* **2019**, *49*, 872–888. [CrossRef]
47. Wang, C.Y. Nonlinear streaming due to the oscillatory stretching of a sheet in a viscous fluid. *Acta Mech.* **1988**, *72*, 261–268. [CrossRef]
48. Abbas, Z.; Wang, Y.; Hayat, T.; Oberlack, M. Hydromagnetic flow in a viscoelastic fluid due to the oscillatory stretching surface. *Int. J. Non-Linear Mech.* **2008**, *43*, 783–793. [CrossRef]
49. Zheng, L.; Jin, X.; Zhang, X.-X.; Zhang, J.-H. Unsteady heat and mass transfer in MHD flow over an oscillatory stretching surface with Soret and Dufour effects. *Acta Mech. Sin.* **2013**, *29*, 667–675. [CrossRef]
50. Liao, S. *Advances in the Homotopy Analysis Method*; World Scientific Pub Co Pte Lt: Singapore, 2013.
51. Turkyilmazoglu, M. Analytic approximate solutions of rotating disk boundary layer flow subject to a uniform suction or injection. *Int. J. Mech. Sci.* **2010**, *52*, 1735–1744. [CrossRef]
52. Turkyilmazoglu, M. The analytical solution of mixed convection heat transfer and fluid flow of a MHD viscoelastic fluid over a permeable stretching surface. *Int. J. Mech. Sci.* **2013**, *77*, 263–268. [CrossRef]
53. Turkyilmazoglu, M. Convergence Accelerating in the Homotopy Analysis Method: A New Approach. *Adv. Appl. Math. Mech.* **2018**, *10*, 925–947. [CrossRef]